Sintering behavior, microstructure and dielectric performance of $BaTiO_3$ with 60-65 wt.% addition of B_2O_3-Bi_2O_3-SiO_2-ZnO glass

Mei-Yu Chen[a], Jari Juuti[a], Heli Jantunen[a]
[a] Microelectronics Research Units, Faculty of Information Technology and Electrical Engineering, University of Oulu, Finland
[*]Corresponding author. Tel. +358 50 350 6982, mei-yu.chen@ oulu.fi; chenmyphy@gmail.com

Abstract

The sintering behaviors and characteristics of a glass-ceramic composite ($BaTiO_3$ with 60-65 wt.% addition of BBSZ) were studied in this paper. The composites showed three-stage phase generation, $Bi_{24}Si_2O_{40}$ at 385-450 ^oC, an intermediate borate phase and $Bi_4Ti_3O_{12}$ at 530 ^oC, ZnO and $BaBi_4Ti_4O_{15}$ at 720 ^oC. High densification was achieved at a sintering temperature of 720 ^oC for the composite with $BaTiO_3$ and 60 wt.% of glass, and at 480 ^oC with 65 wt.% glass addition. The amounts of the phases for different samples were also studied. High permittivity with a relatively low loss value ($\varepsilon_r \sim 116$ and $\tan\delta \sim 0.007$ at 100 kHz) was achieved when the sample having 65 wt.% addition of glass was sintered at 480 ^oC. This sample was also feasible for co-firing with silver electrodes. With a somewhat lower glass addition (60 wt.%), sintering at 720 ^oC generated $BaBi_4Ti_4O_{15}$ phase showing weak ferroelectricity (remanence polarization P_r of 0.17 $\mu C/cm^2$ and a coercive field E_c of 0.85 MV/m with an applied field of 8 MV/m) which also resulted in a higher loss (0.016).

Keywords: glass-ceramic composite, $BaTiO_3$, sintering behavior, microstructure, dielectric/ferroelectric properties

https://doi.org/10.1016/j.jallcom.2017.12.099

1. Introduction

The addition of glass into dielectric ceramics is one of the most efficient and widely used methods of fabricating Low Temperature Co-fired Ceramics (LTCCs). It has been found that dielectric materials with an optimized amount of glass enable low sintering temperatures with feasible dielectric properties [1-4]. George *et al.* [2] reported that the sintering temperature of Li_2CaSiO_4 ceramics can be decreased from 1000 ^oC to 850 ^oC by the addition of different types of glasses, such as $PbO\text{-}B_2O_3\text{-}SiO_2$, $BaO\text{-}B_2O_3\text{-}SiO_2$, $ZnO\text{-}B_2O_3\text{-}SiO_2$, $Li_2O\text{-}B_2O_3\text{-}SiO_2$ and $B_2O_3\text{-}Bi_2O_3\text{-}SiO_2\text{-}ZnO$. Hsi *et al.* [3-4] also found $CaO\text{-}B_2O_3\text{-}SiO_2$ glass beneficial to decrease the sintering temperature of $BaTiO_3$. Among these low melting temperature glasses, lead-free $B_2O_3\text{-}Bi_2O_3\text{-}SiO_2\text{-}ZnO$ (BBSZ) glass is used with various dielectric materials making them feasible for LTCC applications [5-6]. One of the first glass ceramics applied with BBSZ glass for LTCC fabrication was reported in 2001[5]. With the addition of 10 vol.% of BBSZ glass to a 1:1:4 $BaO\text{-}Nd_2O_3\text{-}TiO_2$ microwave ceramic system with a sintering temperature over 1300 ^oC, $BaNd_2Ti_4O_{12}$ was densified at 880 ^oC. Later, many composites were reported utilizing BBSZ addition and sintering temperatures at around 850-950 ^oC, including dielectric and ferrite materials, [5-6]. Peng *et al.* [6] reported that the microwave sintered $Sr_{0.8}La_{0.2}Fe_{11.8}Cu_{0.2}O_{19}$ ferrite with 3-5 wt.% of BBSZ glass sintered at 850-870 ^oC, exhibited excellent ferromagnetic properties (M_s ~ 63.1 emu/g, H_a ~ 17.03 kOe, and H_{ci} ~ 3.59 kOe), and room temperature DC resistivity (ρ_d ~ 16.8×10^9 $\Omega\cdot$cm) suitable for microwave applications. Recently, much attention has been paid to ULTCCs (Ultra-Low Temperature Co-fired Ceramics) with sintering temperatures below 700 ^oC making them feasible for multimaterial and discrete component integrations to create diverse applications. Different ULTCC compositions have also been researched utilizing glass addition. Ju *et al*. reported that the composite with 85 wt.% of $3ZnO–2B_2O_3$ (3Z2B) glass matrix and 15 wt.% of SiO_2 , sintered at 650 ^oC for half an hour , had good dielectric properties (ε_r ~6.1, tan δ ~0.0013 at 1 MHz) [7]. Various

https://doi.org/10.1016/j.jallcom.2017.12.099

fillers, such as $BaTiO_3$ [8] and Al_2O_3 [9], with high amounts of BBSZ glass have also been sintered in the ultra-low sintering temperature region (450 ^oC) for various dielectric applications at kHz-MHz frequencies. The sintering behavior of the $BaTiO_3$-BBSZ composite with both large and small glass content is thus relatively well known. In this study, the sintering behaviors of $BaTiO_3$-BBSZ composite with intermediate addition levels (50- 65 wt.%) were studied. Detailed investigation of the phases and their amounts in the composites below and above the melting point of the BBSZ was performed. The co-firing of silver electrodes with the most feasible samples was studied. Also the microstructures, the phases formed and the dielectric properties at 100 kHz of the sintered samples were investigated and are discussed.

2. Experimental

The BBSZ glass was fabricated as reported earlier [11, 12]. $BaTiO_3$ powder (purity >99.7 %, Alfa Aesar, MA, US) was mixed for 8 hrs with 50, 60 and 65 wt.% BBSZ glass (denoted as A50, A60 and A65) in deionized water without any binder. After drying, the samples were pressed into Ø=10 mm and Ø=20 mm pellet using 200 and 100 MPa, respectively. These samples were sintered at 450 ^oC, 480 ^oC, 500 ^oC, 530 ^oC, 600 ^oC and 720 ^oC for an hour with a heating rate of 3 ^oC/min using a conventional sintering process. The feasibility of co-firing of electrodes was studied by adding 20 wt.% of silver to A60 and A65 composites sintered at 720 ^oC and 480 ^oC, respectively. The sintering behaviors were monitored by a dilatometer (Netzsch DIL402-PC, Germany). The bulk densities of the sintered pellets were measured by the Archimedes method. The microstructures were investigated by FESEM (ZEISS Ultra Plus, Germany) with an energy dispersive spectrometer (EDS). The phases were identified by X-ray diffraction meter (XRD, Rigaku, Co, Kα ~ 1.79 Å, and Cu, Kα ~ 1.54 Å, Tokyo, Japan) and the quantitate analysis of the phases in weight ratio were estimated using Whole Powder Pattern Fitting (WPPF) method by powder diffraction analysis package (PDXL). The dielectric properties at 100 kHz were obtained by a Precision LCR meter (HP

https://doi.org/10.1016/j.jallcom.2017.12.099

4284A, USA).

3. Results and discussion

The dilatometer measurements for samples A50-A65 (Fig. 1) showed that the shrinkage rates increased with increasing amounts of the liquid forming phase of BBSZ glass. This was in good agreement with the previous report [8]. When the sintering temperature approached 800 ^{o}C, the shrinkage of all samples was over 20 %, being about 30 % for the A60 and A65 samples. There were two large shrinkage regions at around 400 ^{o}C and 720 ^{o}C. The A65 sample also showed a swelling at 530 ^{o}C, probably caused by the liquid sintering mechanism reported by German [10]. In this mechanism the swelling of a specimen due to pore formation at prior particle sites has been observed when the liquid forming particles had substantial solubility in the solid during heating. Thus the voids are generated due to the solubility of the liquid. Another possible reason for the observed swelling might be the generation of new phases with higher density. Therefore, more experiments were needed to determine the causes and so the A60 and A65 samples were sintered at

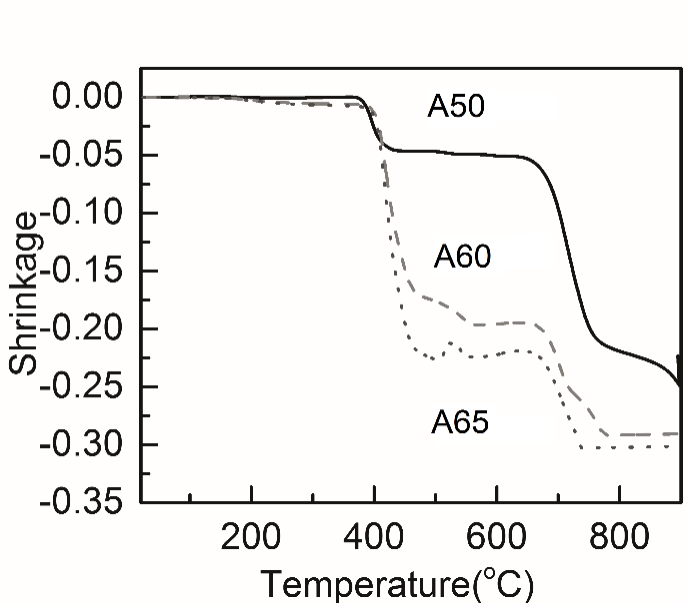

450, 480, 500, 530, 600, and 720 ^{o}C to reveal their microstructures, phases and dielectric properties.

https://doi.org/10.1016/j.jallcom.2017.12.099

Fig. 1 Dilatometry curves of A50-A65 samples.

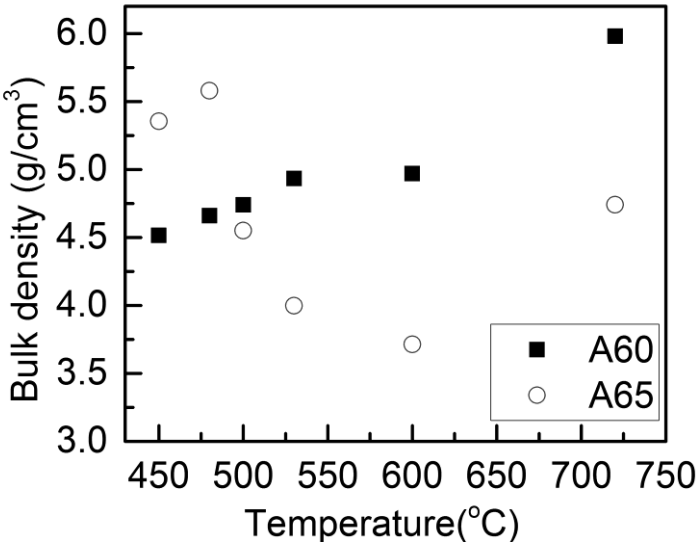

Fig. 2 Bulk densities of A60 and A65 samples sintered at 450 °C to 720 °C.

Fig. 2 shows the bulk densities of the A60 and A65 samples sintered at 450-720 °C. The bulk density of the A60 sample increased almost linearly as a function of sintering temperature and reached a maximum density at 720 °C. Meanwhile, the highest density of the A65 sample was achieved at a sintering temperature of 480 °C.

The XRD patterns of the A60 and A65 samples sintered at 450-720 °C were the same and measurements for the sample A60 are presented in Fig. 3(a)-(b). Thus the sintering mechanism from the point of view of the forming phases seems to be the same for these samples. Only $BaTiO_3$ (peaks denoted with stars) and $Bi_{24}Si_2O_{40}$ (denoted with dots) phases were observed in samples sintered at 450-500 °C (Fig. 3(a)). However, when the sintering temperatures increased to 530 °C (melting point of BBSZ glass), new peaks were detected indicating the existence of a borate $ZnBi_2B_2O_7$ phase and $Bi_4Ti_3O_{12}$ phase. While the sintering temperature was increased to 600 °C, $ZnBi_2B_2O_7$ phase disappeared and ZnO phase appear. Therefore, it seems that BBSZ glass and

https://doi.org/10.1016/j.jallcom.2017.12.099

$BaTiO_3$ particles do not interact with each other below 500 ^oC, but above the melting point of BBSZ glass (530 ^oC) the case is different. Furthermore, the advanced quantitative analysis of XRD spectra (Table I) shows that A65 samples with higher glass content have large amount of $Bi_{24}Si_2O_{40}$ phase compared to A60 sample sintered at the same temperature. Also, the amount of $Bi_{24}Si_2O_{40}$ phase increases with increasing sintering temperature. Nevertheless, the peak intensity associated with $Bi_{24}Si_2O_{40}$ decrease at 530-600 ^oC and finally vanished at 720 ^oC. Besides, at sintering temperature of 720 ^oC, most of $Bi_4Ti_3O_{12}$ phase transforms to $Bi_4BaTi_4O_{15}$ phase. This $BaBi_4Ti_4O_{15}$ phase is observed in similar composite of 50 wt% $BaTiO_3$-50 wt% BBSZ glass [14]. It should be noted that both $Bi_4Ti_3O_{12}$ and $BaBi_4Ti_4O_{15}$ belong to the Aurivillius perovskite family, which is widely used in microwave and optical ceramics and is also attracting attention due to its unique ferroelectric and piezoelectric properties [11-13]. Furthermore, Fig. 3(c) reveals that, with 20 wt.% addition of silver powder, both samples of A60 sintered at 720 ^oC and A65 sintered at 480 ^oC show no existence of extra phase. This indicates that both samples can be integrated with silver electrodes.

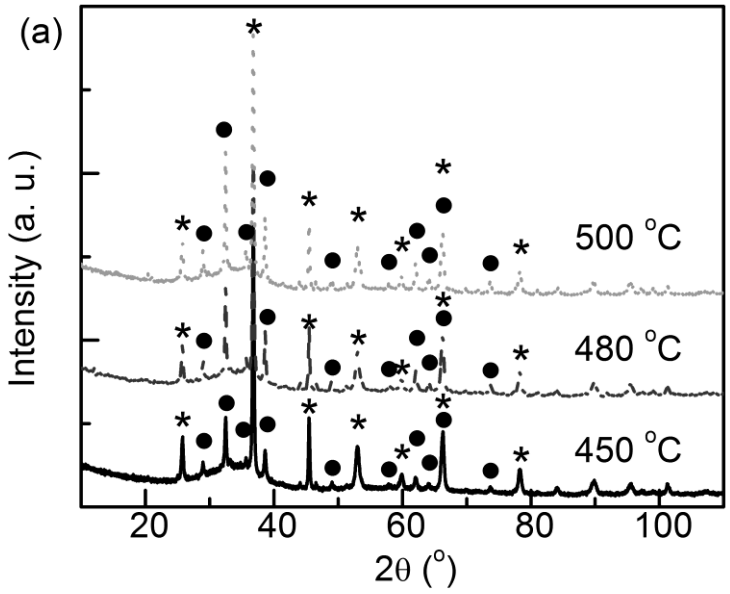

https://doi.org/10.1016/j.jallcom.2017.12.099

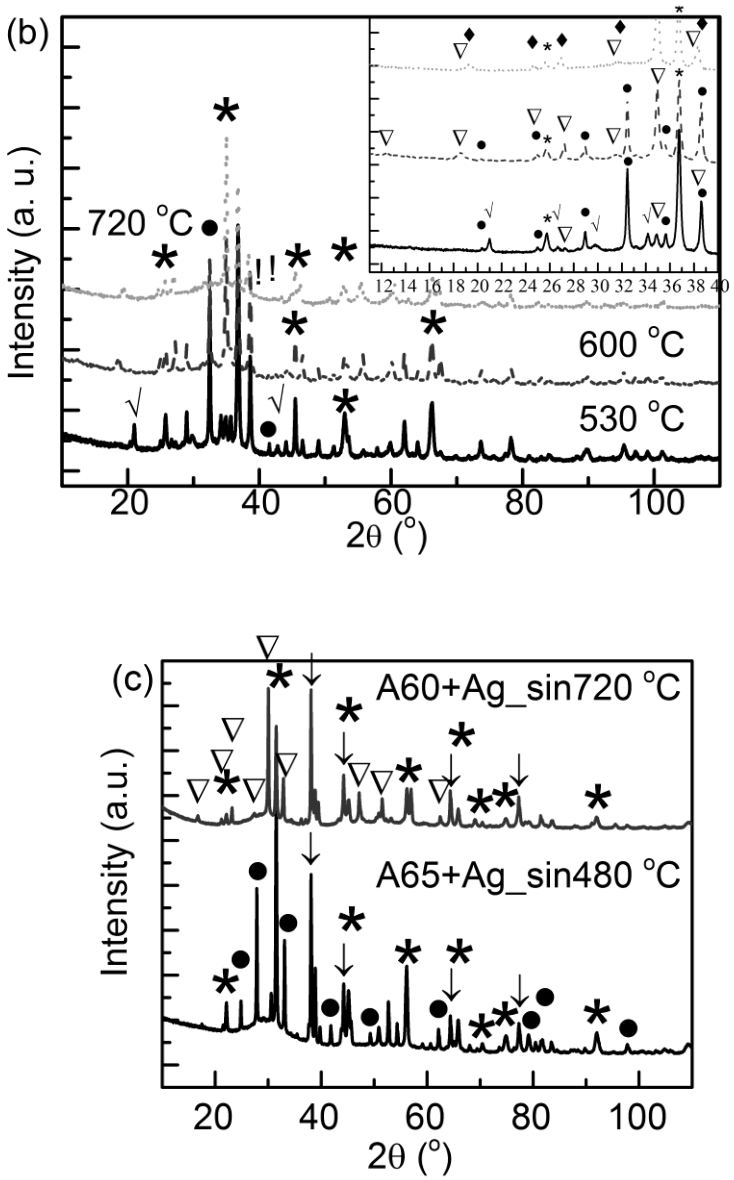

Fig. 3 (a) XRD patterns of sample A60 sintered at 450, 480, 500 °C (b) 530, 600, 720 °C (* refers to $BaTiO_3$, ● refers to $Bi_{24}Si_2O_{40}$, √ to $ZnBi_2B_2O_7$, ∇ to $Bi_4Ti_3O_{12}$, ! to ZnO and ♦ to $BaBi_4Ti_4O_{15}$) and (c) A65 with 20 wt.% Ag sintered 480 °C, and A65 with 20 wt.% Ag sintered at 720 °C(↓ refer to silver)(Cu target).

Table I XRD quantitative phase analysis (in wt.%) of A60 and A65 samples by WPPF method.

Sintering Temperature	Sample	$BaTiO_3$	$Bi_{24}Si_2O_{40}$	$ZnBi_2B_2O_7$	ZnO	$Bi_4Ti_3O_{12}$	$Bi_4BaTi_4O_{15}$
450	A60	85	15	-	-	-	-
	A65	81	19				

https://doi.org/10.1016/j.jallcom.2017.12.099

480	A60	76	24				
	A65	74	26				
500	A60	76	24				
	A65	70	30				
530	A60	54	23	15	-	8	-
	A65	46	25	19	-	10	-
600	A60	43	18	-	4	35	-
	A65	33	22	-	4	41	-
720	A60	45	-	-	4	12	39
	A65	35	-	-	4	8	53

https://doi.org/10.1016/j.jallcom.2017.12.099

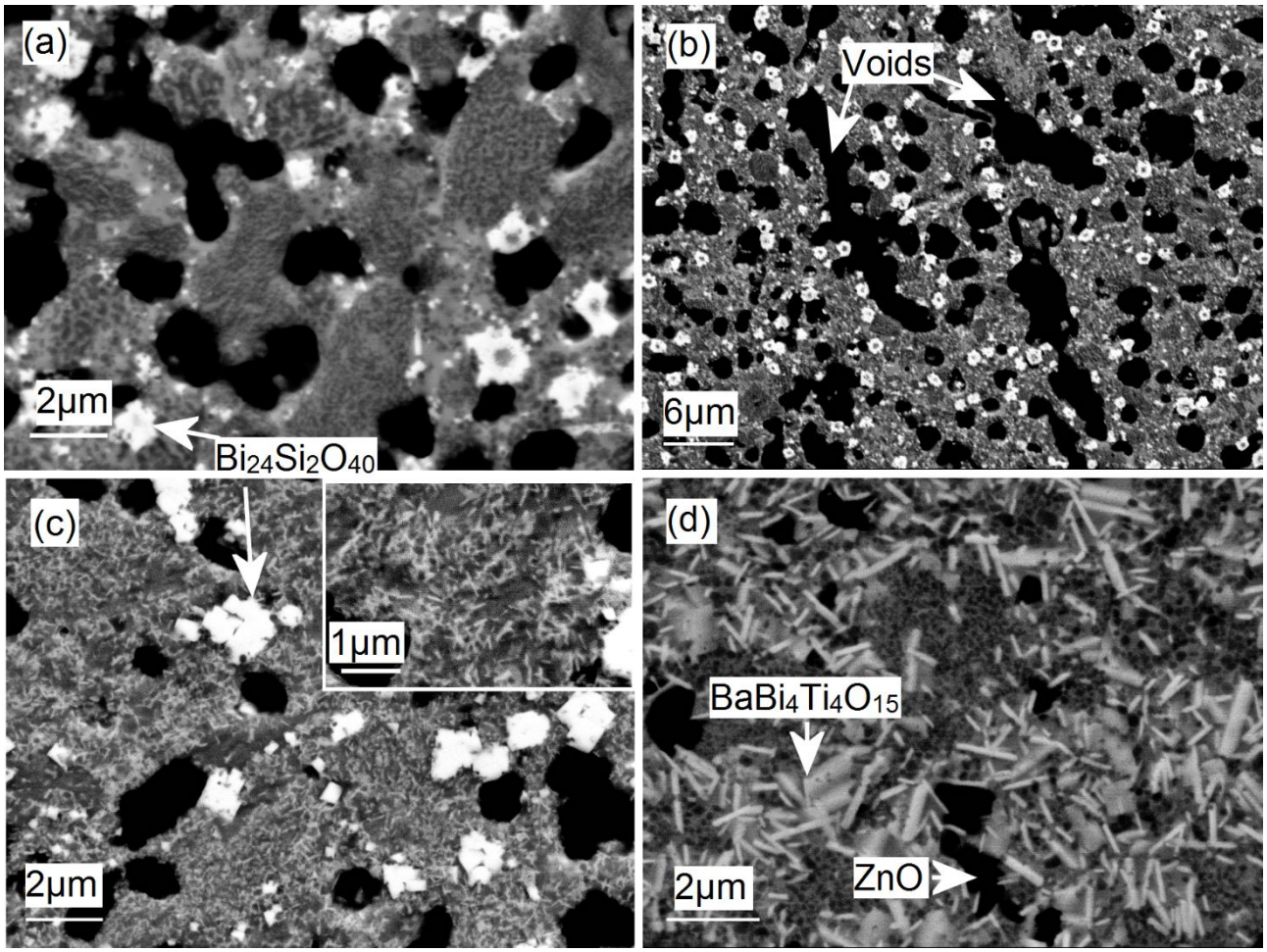

Fig. 4 Backscattered electron images of (a) A60 and (b) A65 at 500 ºC, and A60 sintered at (c) 600 ºC (insert showing the needle type grains) and (d) 720 ºC. (Note: Black color in (a) (b) (c) refers to pores, but in (d) refers to ZnO/Zn rich glass).

https://doi.org/10.1016/j.jallcom.2017.12.099

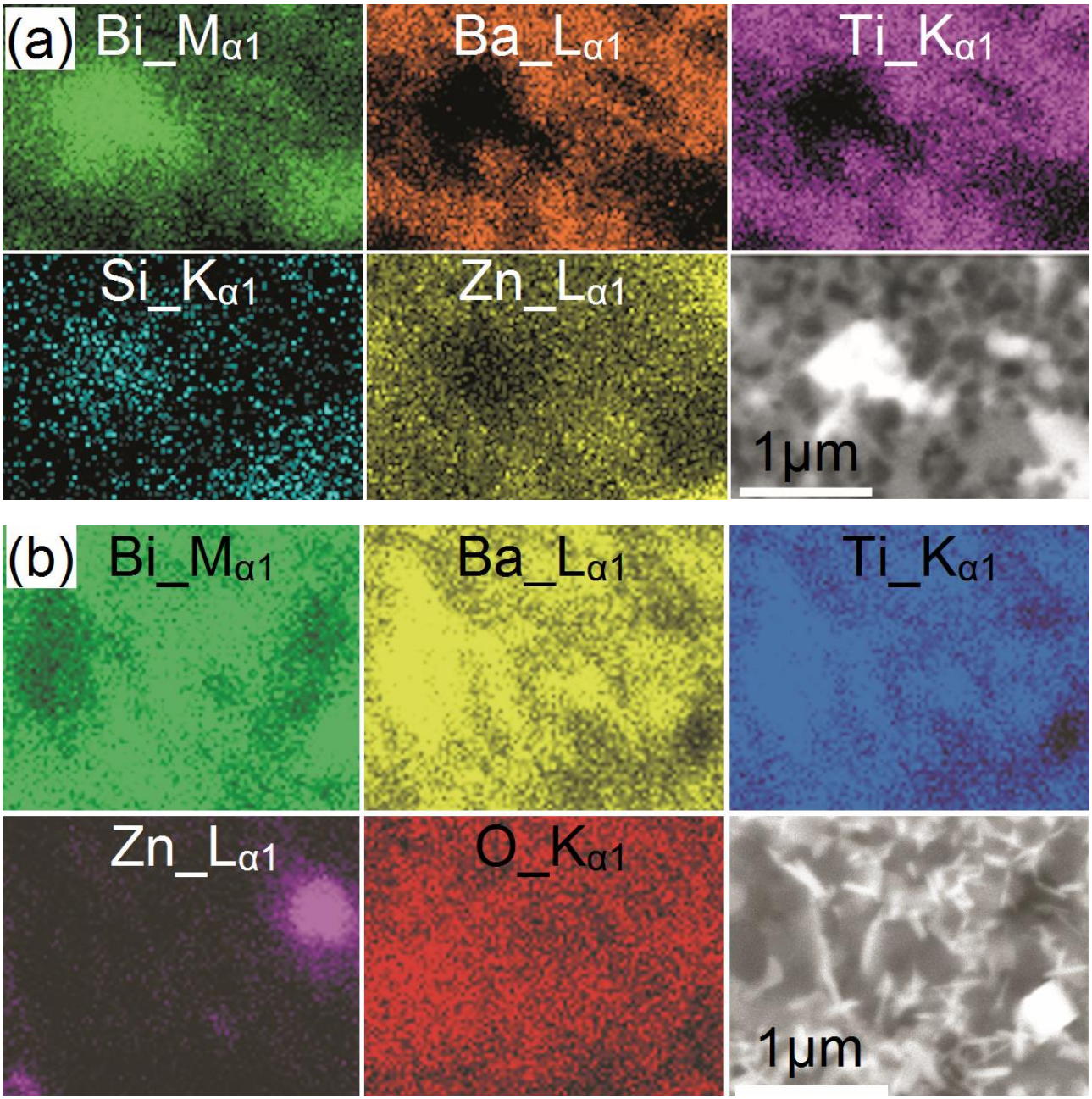

Fig.5 EDS mapping of A60 sintered at (a) 530 °C and (b) 600 °C.

Fig. 4 shows the microstructures of A60 and A65 samples sintered at different temperatures with different phases and black areas which are ZnO/Zn-rich glass cluster in Fig. 4 (d) and pores in the other samples. The EDS analysis of the A60 sample sintered at 500 °C (Fig. 4(a)) relates the dark-grey area to $BaTiO_3$ phase, light-gray to BBSZ and bright white color to $Bi_{24}Si_2O_{40}$ phase. The microstructure of sample A65 sintered at 500 °C (Fig. 4 (b)) shows the same phases. However, the

https://doi.org/10.1016/j.jallcom.2017.12.099

much larger pores coalesce and form meniscus shapes (illustrated at a lower magnification). The EDS map of sample A60 sintered at 530 ^{o}C and 600 ^{o}C are shown in Figure 5. However, due to the low resolution, the $Bi_4Ti_3O_{12}$ phase formed small light gray needles with a length of 230-300 nm (insert in Fig. 4(c)), which can only be clearly observed in the backscattered images. The ZnO/Zn-rich glass cluster can be clearly observed in the samples sintered over 600 ^{o}C (Fig. 5(b)), while Zn element do not cluster in samples sintered at 530 ^{o}C (Fig. 5 (a)). When the sintering temperature reached 720 ^{o}C, the microstructure of the A60 sample totally changed (Fig. 4(d)). The main phases were $BaTiO_3$ (dark grey), $Bi_4Ti_3O_{12}$/$BaBi_4Ti_4O_{15}$ (light grey rod-shape) and ZnO/Zn-rich phase (black area). One of the main differences compared to the other samples was that almost all pores disappeared. The results are in a good agreement with the XRD measurements (Fig. 3).

It seems that when the amount of BBSZ glass was increased (samples A60 and A65, sintering at 500 ^{o}C) the size and the number of the pores also increased. At the same time the amount of $Bi_{24}Si_2O_{40}$ phase increased since it precipitates from the glass and crystallizes, hence decreasing the amount of flowing glass. Thus a dense microstructure was achieved only after the $Bi_{24}Si_2O_{40}$ phase started to react with the remaining glass and $BaTiO_3$, as happened with sample A60 with a sintering temperature of 720 ^{o}C.

Table II Dielectric properties of A60 and A65 sintered at 450-720 ^{o}C at 100 kHz.

@100 kHz	A60		A65	
	ε_r	tan δ	ε_r	tan δ
450	93.1	0.007	103	0.006
480	105	0.007	116	0.007
500	113	0.008	-	-
530	120	0.008	-	-

https://doi.org/10.1016/j.jallcom.2017.12.099

600	101	0.008	-	-
720	115	0.016	-	-

The dielectric properties of A60 and A65 at 100 kHz are shown in Table II. The relative (ε_r) permittivity of A60 increased as a function of sintering temperature and reached its maximum value at 530 ^oC, then decreased at 600 ^oC and increased again at 720 ^oC. The dielectric losses (tan δ) on the other hand showed a value of 0.007-0.008, but sharply increased to 0.016 when the sintering temperature was increased to 720 ^oC. In the case of the A65 sample, the reliable dielectric properties were limited to below 480 ^oC. Comparing these results with those achieved earlier after sintering at 450 ^oC [8], the dielectric properties correlated well taking into account the different dwell times. Thus the permittivity value depended more on the density of the composite than on the amount of $BaTiO_3$ when sintered at below the melting point of glass (530 ^oC). Above that temperature, the crystallization behavior of the samples showed their complexity. The contributions of intermediate $ZnBi_2B_2O_7$ phase, $Ba_{24}Si_2O_{40}$ and $BaTiO_3$, gave ε_r of 120 and a loss of 0.008 at 100 kHz. Additionally the bulk density of A60 increased with sintering temperature. This usually results in an increase in permittivity. However, ε_r decreased to a value of 101 due to the generation and characteristics of the $Bi_4Ti_3O_{12}/BaBi_4Ti_4O_{15}$ phase. With sintering temperatures of 720 ^oC, high densification was achieved, together with a slightly increased permittivity ($\varepsilon_r \sim 115$) but also a rather high loss (tan $\delta \sim 0.016$) was obtained. These dielectric properties can be explained by the removal of large pores and the existence of the $Bi_4Ti_3O_{12}/BaBi_4Ti_4O_{15}$ phase. As mentioned above, these phases belong to the Bi_2O_3-TiO_2 Aurivillius perovskite family, which exhibits highly anisotropic symmetry, so that their dielectric properties can show wide variations between samples [11-12, 15-16]. Cui *et al*. [15] reported that $BaBi_4Ti_4O_{15}$ has tan δ of 0.0135 at 1 kHz. At 1 MHz the value of 0.025 was also reported [16]. Therefore, the observed high loss value of A60 sintered at

https://doi.org/10.1016/j.jallcom.2017.12.099

720 °C was probably due to the dielectric characteristic of $BaBi_4Ti_4O_{15}$.

The temperature dependence of dielectric properties of the A60 sample at 100 kHz sintered at 720 °C are shown in Fig. 6. The permittivity increased with the temperature and reached a maximum value of 157 due to the characteristics of $BaTiO_3$, while the dielectric loss decreased with temperature from 0.016 at room temperature to 0.011 at 150 °C. However, the variation of the permittivity was not greater than 10 % and the loss decreased with temperature meaning that $BaTiO_3$ was not totally dominant in this composite.

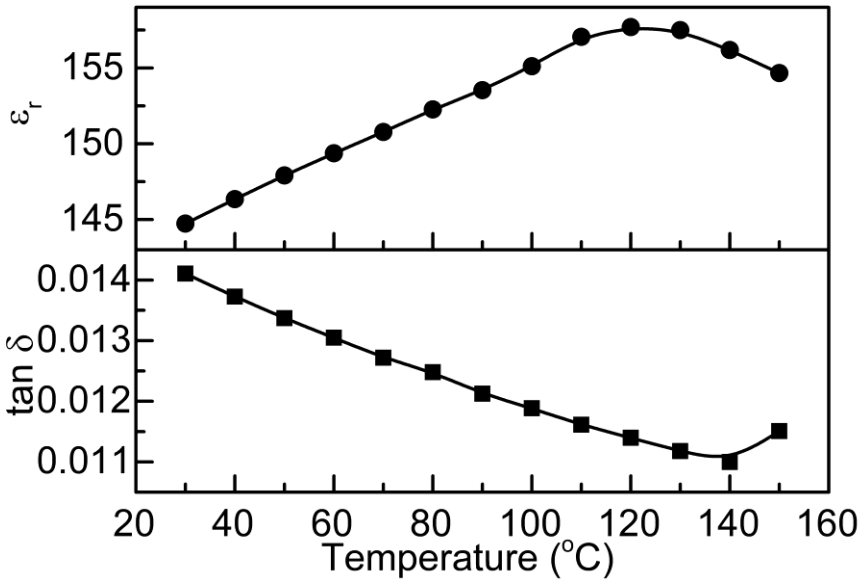

Fig. 6 Temperature dependence of dielectric properties of A60 sintered at 720 °C at 100 kHz.

https://doi.org/10.1016/j.jallcom.2017.12.099

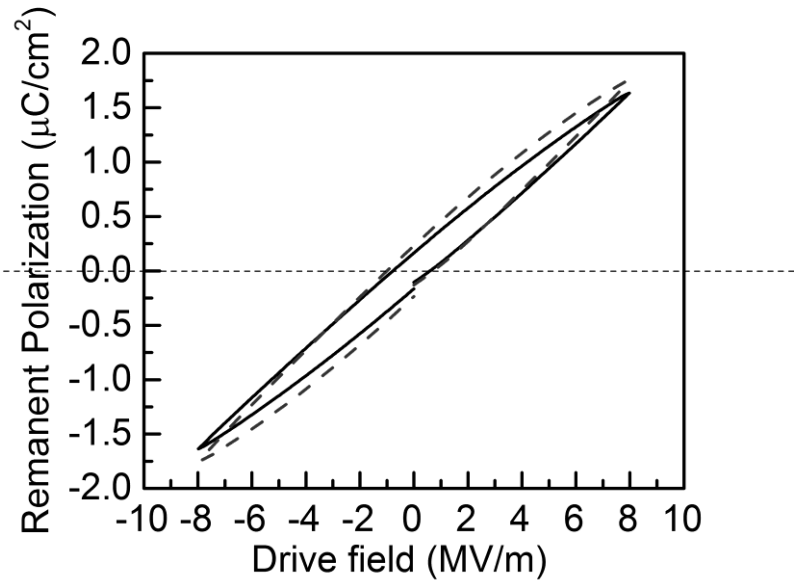

Fig. 7 Hysteresis loops under applied field of 8 MV/m at room temperature (solid line) and 140 °C (dash line) for A60 sintered at 720 °C.

The hysteresis measurements of A60 sintered at 720 °C with an applied field of ~ 8 MV/m are shown in Fig. 7 and Table III. The remanence polarization (P_r) of A60 at room temperature was 0.17 μC/cm^2 and the coercive field (E_c) was 0.85 MV/m. $BaTiO_3$ and $Bi_4BaTi_4O_{15}$ both exhibit ferroelectricity with different Curie temperatures. $BaTiO_3$ transforms to a cubic structures and loses ferroelectricity above 120-130 °C, while $BaBi_4Ti_4O_{15}$ retains ferroelectric properties until its Curie temperature of 417 °C is reached [11-12]. Pure $BaBi_4Ti_4O_{15}$ ceramics prepared by the standard solid-state reaction method have remanence polarization of 5.4 μC/cm^2 and a coercive field of 4.03 MV/m with 8 MV/m applied electric field at room temperature [17]. Additionally, bulk $BaTiO_3$ ceramic has a higher P_r of 8-14 μC/cm^2 and lower E_c of 1.5 MV/m [18]. When the temperature was increased to 140 °C, only $BaBi_4Ti_4O_{15}$ contributed to the ferroelectric properties, and the P_r and E_c values of A60 slightly increased to 0.23 μC/cm^2 and 1.17 MV/m, respectively. The ferroelectricity became more obvious in spite of the absence of the ferroelectric phase of $BaTiO_3$. Typically, the coercive field is expected to decrease at higher temperatures. However, it has previously been

https://doi.org/10.1016/j.jallcom.2017.12.099

observed that in the case of PZT such behavior also depends on the applied electric field and stress state [19], which in this case differed greatly from that of bulk $BaBi_4Ti_4O_{15}$. Thus, the results indicated that $BaBi_4Ti_4O_{15}$ dominated the ferroelectric properties of the A60 sample sintered at 720 ^oC, also explaining the higher dielectric losses.

Table III The remanence polarization P_r and coercive field E_c of A60 sample at room temperature and 140 ^oC

Applied Field=8 (MV/m)	P_r ($\mu C/cm^2$)	E_c (MV/m)
A60@RT	0.17	0.85
A60@140 ^oC	0.23	1.17

In general, the results show that increasing the sintering temperature of A60 indeed improved the densification, but the generation of extra phases affected the dielectric properties of the samples. On the other hand, a higher sintering temperature enhanced ferroelectricity due to the observed $Bi_4Ti_3O_{12}/BaBi_4Ti_4O_{15}$ phase.

Thus, depending on the desired relative permittivity, there are two possible approaches with the BBSZ-$BaTiO_3$ composites with glass loading levels between 50 and 65 wt.%. One is to use 60 wt.% loading and increase the sintering temperature to 720 ^oC , producing a composition with high relative permittivity but also high loss with some level of ferroelectricity. The alternative is to increase the glass content to 65 wt.% and sinter the composite below the glass melting temperature (530 ^oC) if high ε_r and low loss without ferroelectricity are desired. Glass-ceramic composites based on BBSZ glass have a common limitation. The reaction between dielectric and glass cannot be avoided for samples sintered above the melting point of the glass. This result is also observed with other glass-ceramic composites based on BBSZ glass. Induja [20] *et al.* reported that the 40 wt.% Al_2O_3-60 wt. % BBSZ composite sintered at 850-900 ^oC showed the second phase existence of $Bi_{24}Si_2O_{40}$ and $ZnAl_2O_4$. Kim [21] *et al.* also obtained $ZnAl_2O_4$ phase in a similar bismuth-zinc

https://doi.org/10.1016/j.jallcom.2017.12.099

borosilicate glass system (BZBS) with 50 vol.% Al_2O_3 after sintering at 600-950 ^oC. These results indicate that BBSZ glass is relatively reactive above its melting point and it is thus important to understand its characteristics when utilized in composites.

4. Conclusion

In this paper, the sintering behavior, microstructure and dielectric performance of the glass-ceramic composite ($BaTiO_3$ with 60-65 wt.% amount of BBSZ glass) with different sintering temperatures were investigated to understand the properties of this intermediate loading level of BBSZ glass in composites. The dilatometry measurements showed two step shrinkages and swelling in the sample with 65 wt.% amount of glass. This swelling was enhanced due to a new phase generation during heating. The XRD results and WPPF analysis form a new knowledge on existing phases in the composites below and above the melting temperature of the BBSZ glass. The XRD and FESEM results showed the existence of $BaTiO_3$, BBSZ glass and $Bi_{24}Si_2O_{40}$ phases in the samples sintered below 530 ^oC (melting point of BBSZ glass). The intermediate $ZnBi_2B_2O_7$ phase was observed only when sintered at 530 ^oC. Higher sintering temperatures enhanced the generation of $Bi_4Ti_3O_{12}$/$BaBi_4Ti_4O_{15}$ phase and it could be observed in the dense microstructure of A60 sample with $BaTiO_3$ and ZnO rich glass phase after sintering at 720 ^oC. This sample showed high ε_r and tan δ values of 115 and 0.016 at 100 kHz with some ferroelectric behavior. The best dielectric performance was obtained for the A65 sample sintered at 480 °C ($\varepsilon_r \sim 116$ and tan $\delta \sim 0.007$ at 100 kHz) being also feasible with co-fired silver electrodes. Thus this composition could be a potential candidate for ULTCC applications.

5. Acknowledgement:

The work leading to these results has received funding from the European Research Council (ERC) under the European Union's Seventh Framework Programme (FP7/2007-2013) [ERC Grant

https://doi.org/10.1016/j.jallcom.2017.12.099

agreement no. 291132]. Author JJ acknowledges the funding of the Academy of Finland [project numbers 267573 and 273663]. The authors are grateful to the Center of Microscopy and Nanotechnology (CMNT) in the University of Oulu for technological support.

6. Reference

1. E D Zanotto, A bright future for glass-ceramics, *Am. Ceram. Soc. Bull.* **89** (2010) 19-27.

2. S. George, M. T. Sebastian, S. Raman, P. Mohanan, Novel Low Loss, Low Permittivity Glass-Ceramics, *Int. J. Appl. Ceram. Technol.* **8** (2011) 172-179.

3. C-S Hsi, M.-Y. Chen, H Jantunen, F.-C. Hsi, T.-C. Lin, Sintering of titanate based dielectrics doped with lithium fluoride and calcium borosilicate glass, *Mater. Sci.-Poland* **29** (2011) 29-34.

4. C. S. Hsi, Y. C. Chen, H. Jantunen, M. J. Wu, T. C. Lin, Barium titanate based dielectric sintered with a two-stage process, *J. Euro. Ceram. Soc.* **28** (2008) 2581-2588.

5. O. Dernovsek, A. Naeini, G. Preu ,W. Wersing, M. Eberstein, W. A. Schiller, LTCC glass-ceramic composites for microwave application, *J. Euro. Ceram. Soc.* **21** (2001) 1693-1697.

6. L. Peng, L. Li, X. Zhong, R. Wang, X. Tu, Crystal structure and physical properties of microwave sintered $Sr_{1-x}La_xFe_{12-x}Cu_xO_{19}$ (x=0–0.5) ferrites for LTCC applications, *J. Magn. Magn. Mater.* **411** (2016) 62-67.

7. K. Ju, H. Yu, L. Ye, G. Xu, Ultra-low temperature sintering and dielectric properties of SiO_2-filled glass composites, *J. Am. Ceram. Soc.* **96** (2013) 1–6.

8. M.-Y. Chen, J. Juuti, C.-S. Hsi, C.-T. Chia, H. Jantunen, Dielectric $BaTiO_3$–BBSZ glass ceramic composition with ultra-low sintering temperature, *J. Euro. Ceram. Soc.* **35** (2015) 139–144.

9. M.-Y. Chen, J. Juuti, C.-S. Hsi, C.-T. Chia, H. Jantunen, Dielectric Properties of Ultra-Low Sintering Temperature Al_2O_3–BBSZ Glass Composite, *J. Am. Ceram. Soc.* **98** (2015) 1133–1136.

10. R. M. German, P. Suri, S. J. Park, Review: liquid phase sintering, *J Mater Sci* **44** (2009) 1-39.

11. T. Jardiel, A. C. Caballero, M. Villegas, Aurivillius ceramics: $Bi_4Ti_3O_{12}$-based piezoelectrics, *J. Ceram. Soc. Jpn.* **116** (2008) 511-518.

https://doi.org/10.1016/j.jallcom.2017.12.099

12. J. D. Bobic, M. Petrovic, B. D. Stojanovic, Aurivillius $BaBi_4Ti_4O_{15}$ based compound: Structure, synthesis and properties, *Process. Appl. Ceram.* **7** (2013) 97-110.
13. S. R. Emani, A. Joseph, K. C. J. Raju, Optical and microwave properties of $CaBi_4Ti_4O_{15}$ ferroelectric thin films deposited by pulsed laser deposition, AIP conference proceedings 1731 (2016) 080015.
14. M.-Y. Chen, J. Juuti, H. Jantunen, Sintering behavior and characteristics study of $BaTiO_3$ with 50 wt.% of B_2O_3-Bi_2O_3-SiO_2-ZnO glass, *J. Euro. Ceram. Soc*. **37** (2017) 1495-1500.
15. Y. Cui, X. Fu, K. Yan, Effects of Mn-Doping on the Properties of $BaBi_4Ti_4O_{15}$ Bismuth Layer Structured Ceramics, *J. Inorg. Organomet. Polym.* **22** (2012) 82–85.
16. C .L. Diao, J. B. Xu, H. W. Zheng, L. Fang, Y. Z. Gu, W.F. Zhang, Dielectric and piezoelectric properties of cerium modified $BaBi_4Ti_4O_{15}$ ceramics, *Ceram. Int.* **39** (2013) 6991-6995.
17. P. Fang, H. Fan, Z. Xi, W. Chen, Studies of structural and electrical properties on four-layers Aurivillius phase $BaBi_4Ti_4O_{15}$, *Solid State Commun.*, **152** (2012) 979–983.
18. B. Jafee, W. R. Cook and H. Jafee, Piezoelectric Ceramics, *Academic Press London and New York* (1971), 78.
19. J. Juuti, H. Jantunen, V.-P. Moilanen, S. Leppävuori, Poling conditions of pre-stressed piezoelectric actuators and their displacement, *J. Electroceram.* **15** (2005) 57-64.
20. I. J. Induja, P. Abhilash, S. Arun, K. P. Suredran, M. T. Sebastian, LTCC tapes based on Al_2O_3–BBSZ glass with improved thermal conductivity, *Ceram. Int.* **41** (2015) 13572-13581.
21. K. S. Kim, S. H. Shim, S. Kim, S. O. Yoon, Microwave dielectric properties of ceramic/glass composites with bismuth-zinc borosilicate glass, *J. Ceram. Proc. Res.* **11** (2010) 47-51.

https://doi.org/10.1016/j.jallcom.2017.12.099